RESEARCH

Open Access

Isolation of curcumin from Lakadong turmeric of Meghalaya and development of its PLGA-Cur-NS loaded nanogel for potential anti-inflammatory and cutaneous wound healing activity in Wistar rats

Sanjib K. Sarma[1], Uloopi Dutta[1], Alakesh Bharali[1,2], Suman Kumar[1], Sunayna Baruah[1,3], Himangshu Sarma[1,4], Damiki Laloo[1,5*] and Bhanu P. Sahu[1,2*]

Abstract

Background Lakadong turmeric (LKD) from Meghalaya, India, boasts high curcumin levels, but lacks scientific study. Moreover, Curcumin's poor solubility hinders its clinical use in inflammation and wound healing. This study isolated curcumin from LKD, forming a PLGA nanosuspension-based nanogel and explored for its potential anti-inflammatory and cutaneous wound healing activity in Wistar rats.

Methodology The LKD rhizome was successively extracted by soxhlet using chloroform, hexane, ethyl acetate and methanol and their total phenolic content and antioxidant property was determined. Chloroform extract was loaded in column chromatography and curcumin was isolated, purified and characterized by FTIR, NMR, DSC, MS and HPTLC and its purity was analyzed by HPLC. The isolated curcumin was loaded into PLGA nanosuspensions by nanoprecipitation method followed by conversion to carbopol based Nanogel. The nanogels were characterized physicochemically and the drug permeation was observed. The optimized nanogel was evaluated for its anti-inflammatory and cutaneous wound healing activity by carrageenan-induced paw edema and excision wound model in albino Wistar rats divided in five groups and treated with plain carbopol gel, marketed turmeric cream and Cur NS nanogel (0.6% w/w equivalent curcumin each).

Results Results depicted that the chloroform extract showed the presence of a considerable amount of phenolics with 50-60% yield of curcumin. HPLC analysis depicted that the LKD curcumin had higher purity when compared to standard curcumin. Homogenous curcumin nanosuspensions were obtained with size 150 ± 50 nm and PDI 0.2 ± 0.1. The Cur-NS-nanogel showed satisfactory physical property, drug loading and stability. Ex vivo permeation studies in rats showed controlled permeation with steady state flux of 21.28 ± 0.23 µg/cm^2/hr in 24 h. Topical intervention with Cur-NS-nanogel (0.6%) significantly ($p < 0.05$) decreased the paw volume by 43.97% in the 3rd hour and 72.19% on the 4th hour. Furthermore, the cutaneous wound healing property of Cur-NS-nanogel when compared

---

*Correspondence:
Damiki Laloo
damiki.laloo@gmail.com
Bhanu P. Sahu
drbpsahu@gmail.com
Full list of author information is available at the end of the article

to negative control rats showed a substantial ($p < 0.05$) reduction in the percentage wound contraction from 5 to 20th days.

Conclusion LKD showed high curcumin content with significant antioxidant effects. LKD curcumin loaded into stable nanogel depicted safe and controlled skin permeability with promising cutaneous wound healing and anti-inflammatory activity in experimental rats.

Keywords Curcumin, Lakadong turmeric, Nanogel, Antioxidant, Anti-inflammatory, Wound healing

Background

Curcumin, obtained from rhizome of *Curcuma longa* L. is a linear diarylheptanoid with excellent medicinal properties [1]. It is a low molecular weight polyphenol (1,7-bis(4-hydroxy-3-methoxyphenyl)-1,6-heptadien-3,5-dione) and is lipophilic in nature. Curcumin content varies with various lines of *C. longa* due to hybridization and introgression with other species of *Curcuma* [2]. Lakadong Turmeric is regarded as one of the greatest turmeric kinds in the world due to its 6.8 to 7.5 percent curcumin concentration [3–5]. This type of turmeric is native to Meghalaya's Jaintia Hills, specifically the Lakadong region [5]. While there have been reports highlighting curcumin's anti-inflammatory and antioxidant activities, there is a limited amount of information available regarding curcumin derived from lakadong turmeric of Meghalaya. [6]. Hence, there is a need to have more scientific reports on Lakadong turmeric based curcumin considering its better quality and yield which gives it huge potential for nutraceutical and pharmaceutical application.

One major limitation of curcumin, restricting its successful application is its poor bioavailability due to its less solubility [7]. In recent years, nano drug delivery systems have significantly enhanced the bioavailability and aqueous solubility of curcumin. Nanosuspensions (NSs) due to its various advantages are the most clinically successful nanoformulation in enhancing the solubility of poorly soluble drugs [8]. However**,** the advantages of NSs, that includes its high reactivity, great capacity and small size, may also inflict toxic effects on cells compared to its microsized counterparts [9, 10]. Hence, a suitable carrier as PLGA based NS loaded carbopol nanogel may be a better preparation with reduced nanotoxicity. Moreover this nanogel may also result in a more controlled therapy which is essential for its anti-inflammatory and wound healing effect.

Wounds typically represent physical injuries that cause the loss of epithelial integrity as well as the disturbance of normal structure and function of the skin and its tissues that underneath it. Many physiological events occur throughout the wound healing process, including clothing, coagulation, inflammation, and the formation of new tissues. Any drug that has the ability

to accelerate these activities is termed a wound healing promoter, and turmeric (*Curcuma longa* L.) along with its bioactive ingredient curcumin have been scientifically employed to treat wounds. Additionally, curcumin has also been shown to increase granulation in bodily tissue, including increased cellular content and new vascularization, as well as the process of wound re-epithelialization [11, 12]. However, the poor solubility of curcumin results in limited skin permeation through the stratum corneum (SC), and is a major limitation for its topical application in cutaneous wound healing [11]. Hence, development of a topical delivery system that can enhance the solubility of curcumin and promote its permeation through the skin is very essential. There are reports of cutaneous wound healing activity of nanogels based on nanoemulsion coupled with ultrasonication [12], but there are no reports of nanosuspension based nanogel, which are simpler in preparation and use lesser surfactants and cosurfactants in formulation, which may otherwise irritate the wounds. Hence in the present study a superior quality curcumin was extracted, isolated and purified from Lakadong turmeric with better yield as compared to other reported yields of turmeric. The isolated curcumin was characterized by various analytical techniques for its identity and purity. The antioxidant and anti-inflammatory efficacy of the obtained extracts were observed. PLGA based nanosuspensions were then prepared using this isolated curcumin by nanoprecipitation technique. The Cur-NS was then converted to nanogel using carbopol for topical application in cutaneous wound healing and inflammation.

Methods

Materials

Pure curcumin (95% purity) was procured from SRL, India. Various solvents including chloroform, hexane, ethyl acetate, and methanol were obtained from RANKEM, India. Poly Vinyl alcohol (PVA) was sourced from Sigma Aldrich, while PLGA and carbopol 940 were obtained from Yarrow Chem, Mumbai. Triethanolamine oleate was purchased from SRL. All chemicals were of analytical grade, and demineralized water was used.

Sarma *et al. Future Journal of Pharmaceutical Sciences*   (2023) 9:85

Page 3 of 21

Plant material, processing and extraction process

Fresh Lakadong turmeric (LKD) rhizomes were collected from the Lakadong region in Meghalaya, India (Location: 25° 11′ 0″ North, 92° 17′ 0″ East). The plant material was authenticated at the Botanical Survey of India, Shillong, Meghalaya (India) and a voucher specimen (Specimen number. GIPS/2018/003) was preserved for future reference at the Central Museum of GIPS, Guwahati, India. The rhizomes were cleaned, dried, and ground into coarse powder. The homogeneous powdered material (1 kg) was subjected to successive extraction for 72 h using solvents (2.5 L) of increasing polarity (hexane, chloroform, ethyl acetate, and methanol) in a Soxhlet apparatus. The extracts obtained were filtered, concentrated using reduced pressure and labeled as hexane extract (LKDHE), chloroform extract (LKDCH), ethyl acetate extract (LKDEA), and methanol extract (LKDME).

Residual solvents in extracts by gas chromatography

The collected extracts were analyzed for residual solvent content using Gas Chromatography (GC) with a Headspace system (Clarus 690 Perkin Elmer). The injection Volume sampling rate was maintained at 12,50000pts/s with initial oven temperature at 40̊ C for 2 min followed by GC run (Ramp 1 at 5.0 deg/min to 100 deg/min hold for 1 min and Ramp 2 10.0 deg/min to 150 deg/min with hold time of 0.00 min), offset at 100 µV. Extract samples were placed in vials, and the GC run was executed following the specified procedure (Fig. 1). The outcomes are displayed in Additional file 1: Fig. S1.

Physical evaluations and phytochemical studies of the LKD successive extracts

Physical properties of the LKD successive extracts

Various physical parameters were evaluated on the extracts including testing for organoleptic characters, nature of the extract, percentage yield; pH and solubility testing were determined [13].

Phytochemical evaluations and analytical process of curcumin from LKD

Preliminary phytochemical screening, thin layer chromatography and quantification of total phenolic content

Phytochemical screening of the LKD successive extracts was conducted to identify various classes of phytochemicals [14]. Prominent phytochemical classes that produced positive test results underwent further verification using Thin-Layer Chromatography (TLC) methods. For extracts abundant in curcuminoids, TLC analysis was executed following established protocols [15]. The procedure encompassed preparing sample extracts for analysis, selecting the stationary phase, optimizing the mobile phase, developing the chromatogram, and spotting detection, all in accordance with established guidelines. The stationary phase for TLC employed pre-coated silica gel 60 F_{254} aluminum sheets (Merck Ltd.), while the mobile phase was composed of a mixture of chloroform and methanol in a 9:1 ratio. Subsequently, the TLC plates were observed using short UV light (264 nm), long UV light (366 nm), and visible light, both before and after applying the detecting reagent. Furthermore, the optimization of High-Performance Thin-Layer Chromatography (HPTLC) fingerprinting and the analysis of the curcumin-rich crude fraction after isolation via column chromatography were performed using HPTLC CAMAG equipment, which included the Linomat V sample applicator, CAMAG TLC visualizer, and WINCATS 4 software.

Furthermore, based on the results of the preliminary phytochemical screening and TLC analysis, further studies were conducted for the total phenolic and tannin content estimation using a UV–Visible spectrophotometer (Shimadzu-AA6300). The total phenolic content and total tannin content were determined using the Folin-Ciocalteu method with certain modifications [16]. Sampling was done by preparing all the successive extracts at concentration of 1 mg/mL. A series of dilution in the concentration range of 0.02–0.10 mg/mL was prepared for tannic acid (1 mg/mL stock solution) taken as reference standard. The total phenolics (TP), total simple phenolics (TSP) and total tannin content (TC) were estimated using the reported methods. All estimations were performed in triplicates and were statistically expressed as Mean ± S.E.M using linear regression equation.

Isolation and characterization of curcumin from LKD

The analysis of the chloroform extract (LKDCH) through TLC and HPTLC confirmed a notable presence of curcumin. Consequently, an attempt was undertaken to isolate curcumin from this extract, employing a column chromatography approach. The wet packing method was adopted, wherein the column was packed with silica gel (#60–120 mesh, column grade, Merck Ltd.), combined with exceptionally pure chloroform. LKDCH (50 g) was absorbed in chloroform and introduced into the column. The elution process was executed by employing a gradient mixture of methanol (MeOH) and chloroform ($CHCl_3$), with a progressively increasing proportion of MeOH within $CHCl_3$. The gradient levels were as follows: 1%, 2.5%, 5%, 7.5%, 10%, 15%, 20%, 40%, 60%, 80%, and finally, 100%. The eluates were collected in 25 mL fractions. Similar R_f values led to the pooling of corresponding eluates, which were subsequently concentrated using a rotary evaporator. The procedure yielded 105 fractions.

Sarma *et al. Future Journal of Pharmaceutical Sciences*   (2023) 9:85

Page 4 of 21
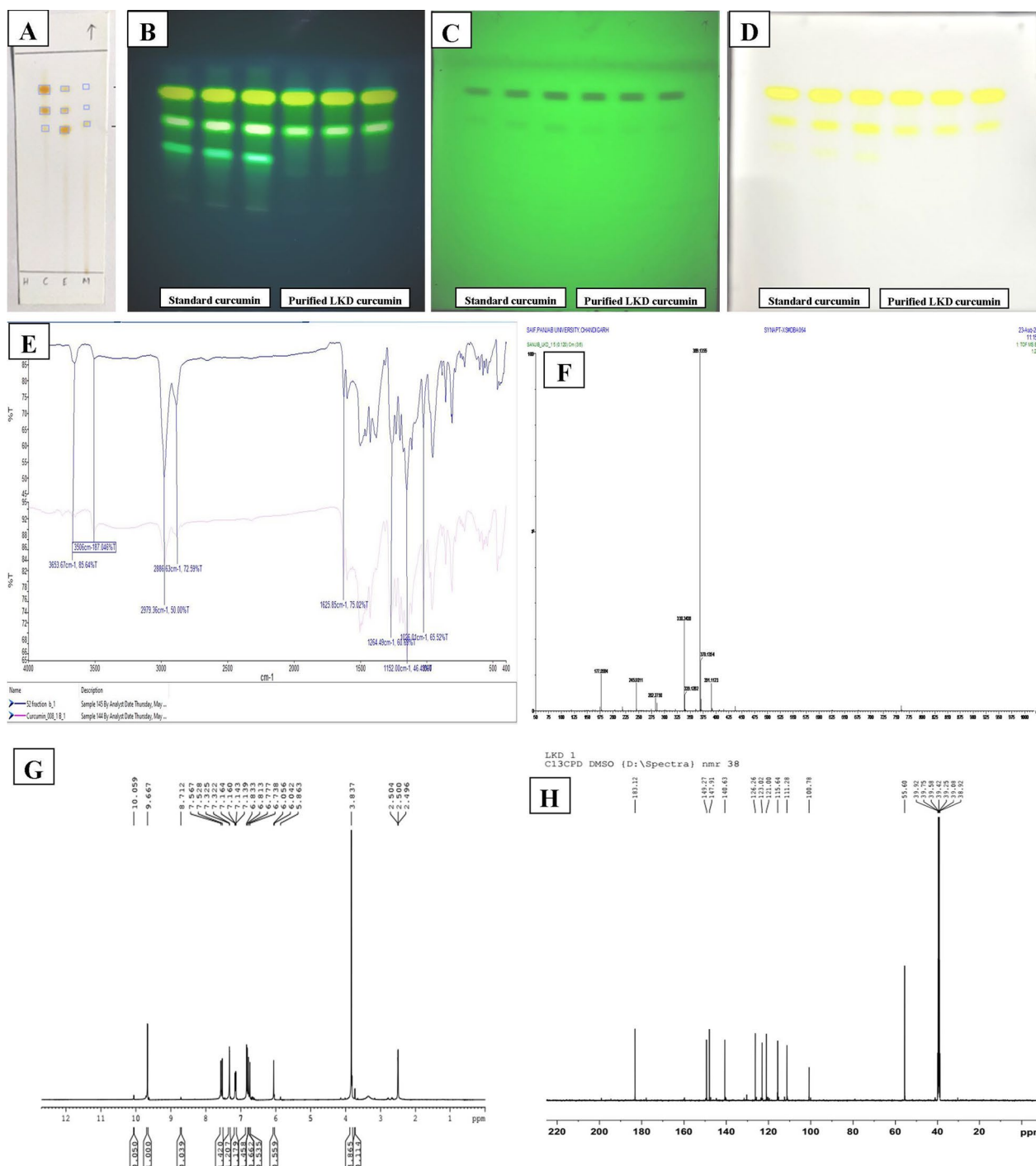
Fig. 1 Phytochemical evaluation of LKD extracts and characterization of curcumin. **A**: TLC chromatogram of LKD successive extracts; **B**, **C**, **D**: HPTLC fingerprinting of isolated curcumin from LKDCH **E** FTIR fingerprinting of purified LKD curcumin **F** MS spectra **G** ^{1}H NMR of purified LKD curcumin **H** ^{13}C NMR of purified LKD curcumin

Notably, fractions 50–55 exhibited distinct yellow single spots of curcumin, which were then combined and subjected to concentration. To enhance its purity, curcumin was purified through recrystallization in 100% acetone and stored at room temperature.

Sarma *et al. Future Journal of Pharmaceutical Sciences*   (2023) 9:85

Page 5 of 21

The characterization and interpretation of the structure of the isolated curcumin was analyzed by sophisticated spectrometric techniques including FTIR (Bruker Alpha), ^{1}HNMR and ^{13}CNMR (Bruker Avance Neo 500 MHz FT-NMR spectrometer), Mass spectrometer (Waters Corporation MALDI-TOF SYNAPT XS HD Mass spectrometer) [17].

Differential scanning calorimetry (DSC)

The DSC 3 instrument (Mettler Toledo; Model no-ME-5140313) was employed to examine the melting point behavior of both the isolated and purified curcumin, as well as the standard curcumin. Samples were positioned in aluminum pans and subjected to scanning at a rate of 10 °C per minute within the temperature range of 20 °C to 300 °C under an inert nitrogen gas environment. For confirming the identity and purity of the isolated curcumin, a comparison was made between the endothermic peak of the isolated curcumin and that of the standard curcumin [18].

HPLC analysis for determination of the purity of isolated curcumin

The purity of isolated Curcumin from Lakadong Turmeric extracts was determined by HPLC (Arc HPLC, Waters). The HPLC System consisted of a chromatographic pump, Injector, and UV detector. For HPLC separation, a reversed-phase C-18 column was used. The mobile phase was composed of acetonitrile-acidic Water (pH 3 adjusted by acetic acid) (80:20v/v) at a flow rate of 1 m/min. The run time was 10 min and the detection wavelength was set at 425 nm. The mobile phase was filtered using a 0.2 nm millipore membrane filter. The sample injection volume was set at 20 µl. The purity was determined by comparing it with a chromatogram of the standard curcumin from SRL, India (95% Purity) [8]. The result is shown in Fig. 2.

Nuclear magnetic resonance (NMR)

The chemical identity of the LKCH isolated curcumin was further confirmed by proton NMR spectrum usingHigh
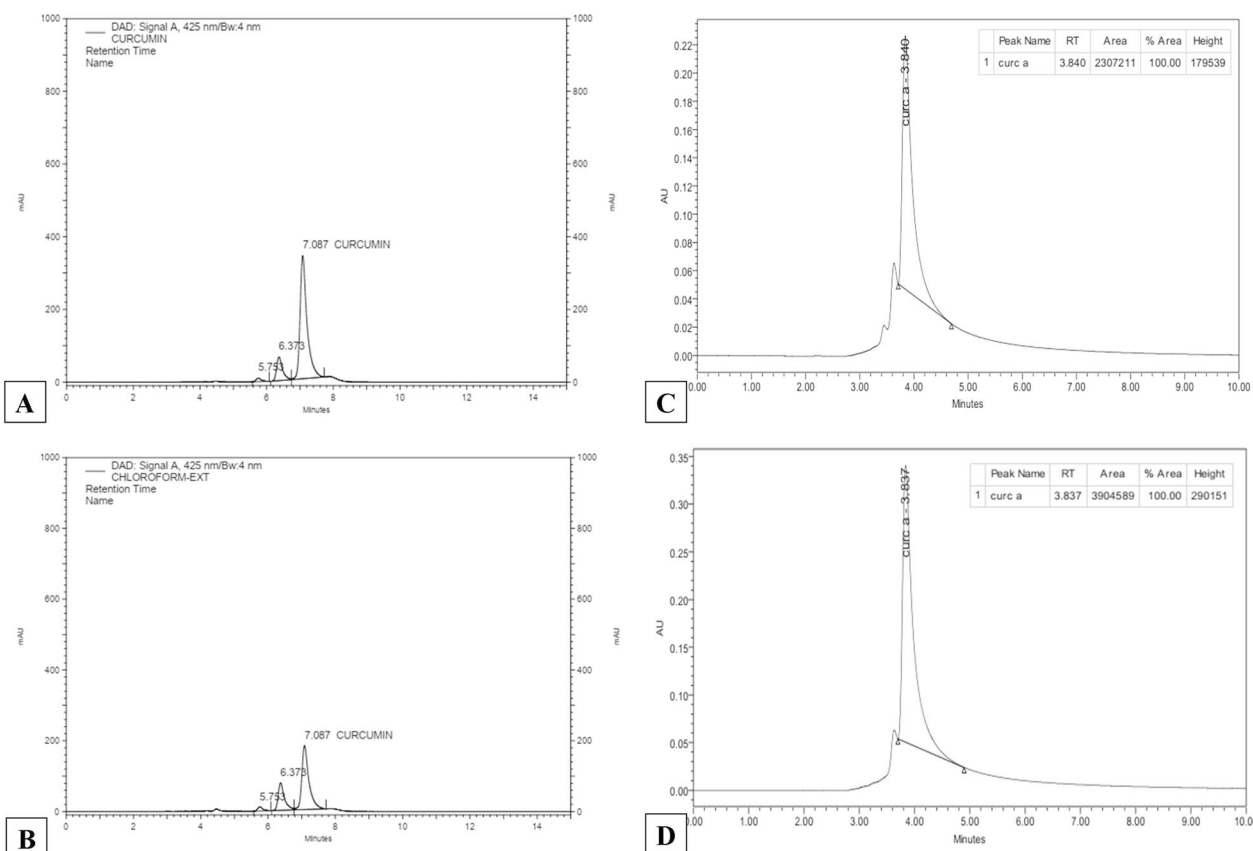
Fig. 2 HPLC chromatogram of curcumin. **A**: Curcumin standard; **B**: Curcumin in LKDCH and purity of isolated curcumin from LKDCH; **C**: Curcumin standard; **D** Curcumin isolated from LKDCH

Resolution Multinuclear FT-NMR Spectrometer (ECX400 -Jeol 400 MHz, Japan). The samples were dissolved in dimethyl sulfoxide d6 (DMSO d6) as solvent. 20 µl of tetramethylsilane (TMS) was added to the sample solution as the internal reference. Chemical shifts observed were reported in parts per million (ppm) relative to expression of tetramethylsilane (TMS) in δ units, and the spin multiplicities were obtained as s(singlet) and d (doublet) [17].

Fourier-transform infrared spectroscopy (FTIR)
The IR spectrum of isolated LKDCH curcumin was further compared with that of the standard curcumin used to determine its structural identity using FT-IR spectrophotometer (Perkin Elmer Model: L1600400 Spectrum Two Ft-IR/DTGS). The samples were placed directly in a KBr-coated pan and scanned at 400 to 4000 cm^{-1} [18].
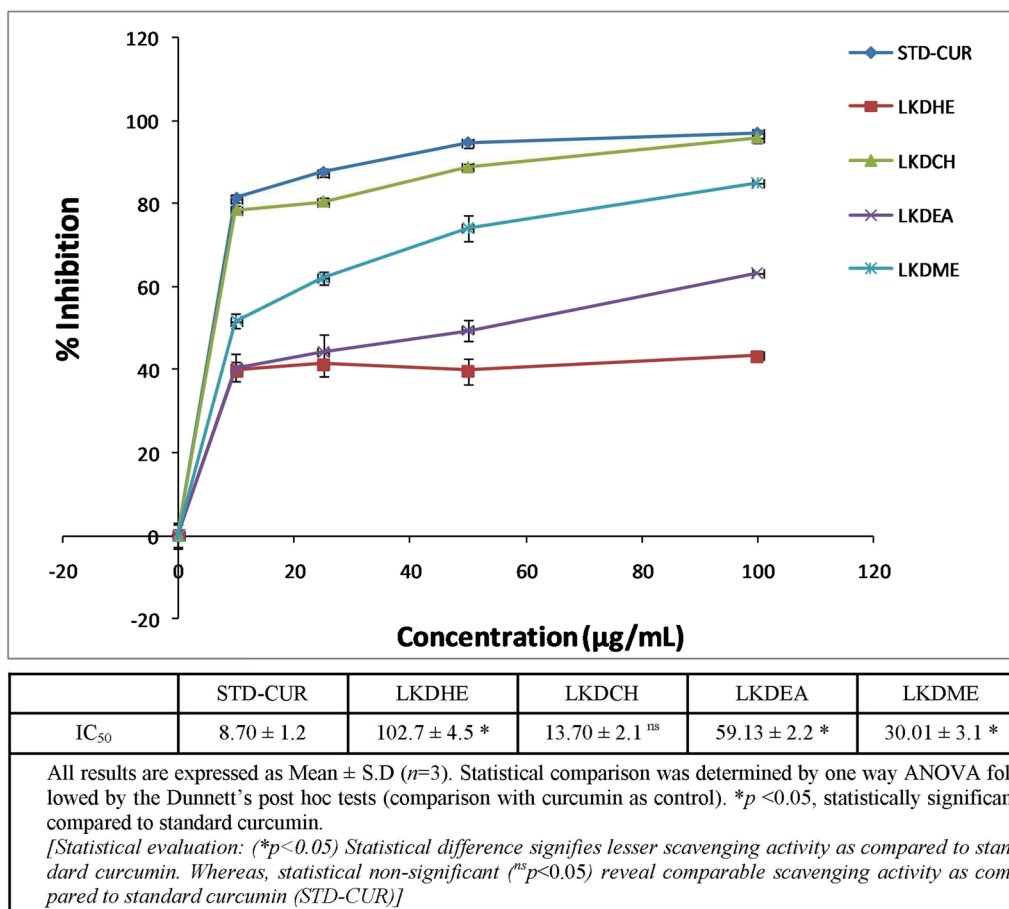
DPPH free radical scavenging activity
The standard approach was used to test the free radical scavenging ability of PFSEs against DPPH (1, 1 diphenyl-2-picrylhydrazyl) with minor modifications [19]. Aliquot series of dilutions (25–200 g/mL) of both LKD successive extracts and reference standard ascorbic acid were made from the stock solution (1 mg/mL). The reaction was started by combining individually the specific concentration of series of dilutions of LKD extracts and standard solution of ascorbic acid (25–200 g/mL) with 5 mL of a DPPH solution that had been prepared in methanol at a concentration of 100 mM/mL. After 30 min of dark incubation, the reaction mixtures were tested for absorbance at 517 nm

$$\% \text{ Inhibition} = [(A_0 - A_1)/A_0] \times 100$$

The absorbance of control solution is denoted by "A_0" in this equation, while the absorbance of test sample is denoted by "A_1". The IC_{50} was determined using ascorbic acid as a control and the regression equation by plotting the percentage inhibition against the relevant values. The results are shown in Fig. 3.

	STD-CUR	LKDHE	LKDCH	LKDEA	LKDME
IC_{50}	8.70 ± 1.2	102.7 ± 4.5 *	13.70 ± 2.1 [ns]	59.13 ± 2.2 *	30.01 ± 3.1 *

All results are expressed as Mean ± S.D (*n*=3). Statistical comparison was determined by one way ANOVA followed by the Dunnett's post hoc tests (comparison with curcumin as control). *p <0.05, statistically significant compared to standard curcumin.
[Statistical evaluation: (*p<0.05) Statistical difference signifies lesser scavenging activity as compared to standard curcumin. Whereas, statistical non-significant (^{ns}p<0.05) reveal comparable scavenging activity as compared to standard curcumin (STD-CUR)]

Fig. 3 DPPH radical scavenging activity of the LKD successive extracts

Sarma *et al. Future Journal of Pharmaceutical Sciences* (2023) 9:85

Page 7 of 21

HRBC membrane stabilization assay

HRBC membrane stabilization assay was performed to evaluate the anti-inflammatory efficacy [20]. Blood samples were mixed equally with sterile Alsever medium containing (2% (w/v) dextrose, 0.8% sodium citrate, 0.5% citric acid, and 0.42% sodium chloride in water). The blood was then centrifuged for an additional 10 min at a higher speed of 3000 rpm. Isosaline (0.85%, pH 7.2) was used to clean the packed cells after which a 10% (v/v) solution of isosaline was made. The secondary metabolite obtained from the plant extract, 1 mL of phosphate buffer pH 7.4 (0.15 M), 2 mL of 0.36% hyposaline, and 0.5 mL of HRBC suspension were all included in the test mixture. As a benchmark medication, diclofenac was employed. Distilled water(2 mL) was used as the control in place of the hyposaline solution. The test mixtures were centrifuged at 3000 rpm for 10 min after being incubated for 30 min at 37° C. Using a UV–Visible spectrophotometer set to 560 nm, the amount of hemoglobin in the supernatant was calculated [21]. The following equation was used to compute the percentage of hemolysis:

$$\text{Hemolysis (\%)} = \left(\text{Optical density of test sample} / \text{Optical density of control}\right) \times 100$$

$$\text{Protection (\%)} = 100 - \left[\left(\text{Optical density of test sample} / \text{Optical density of control}\right) \times 100\right]$$

Preparation of nanosuspension by precipitation-sonication method

Nanosuspensions were prepared with the Curcumin isolated from LKDCH using the precipitation-sonication method [22]. Briefly, the drug was added in 2 ml acetone and vortexed.To this solution PLGA was added to get the organic phase. The PLGA-CUR solution was then injected rapidly to 20 ml of previously prepared PVA solution followed by sonication for 10 min at 60 amplitude and 0.6 cycles. These precipitated nanosuspensions were then kept overnight under stirring to evaporate out the organic solvent.

Characterisation and optimisation of Curcumin nanosuspensions (Cur-NS)

Measurement of particle size and polydispersity index

The average size and the polydispersity index (PDI) of the Cur-NS were measured using dynamic light scattering (DLS) method after suitable dilution (Zetasizer, Malvern Nano S90). All the measurement were done in triplicate at 25 °C with a scattering angle of 90°. The zeta potential of the preparations was also measured by electrophoretic mobility method using clear disposable zeta cell (Zetasizer Ver. V 2 2 Malvern) [23].
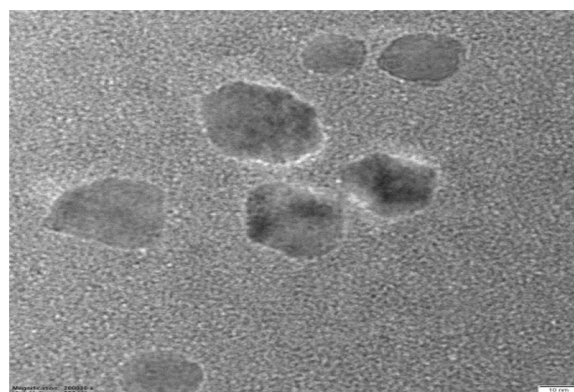
Fig. 4 TEM photomicrograph of Curcumin Nanosuspension

Transmission electron microscopy (TEM)

The size and morphology of the nanoparticles were further evaluated by TEM. The Cur-NS was added drop wise onto a copper grid with a carbon coating of 400 mesh. The grid was stained for 20 min with a solution of phosphotungsten acid (2 percent, w/v) after being tapped with filter paper to remove extra water about 15 min after nanoparticle deposition and air dried. The TEM images were then obtained using TEM (JEM-2100 PLUS (HR), JEOL) at 200,000 × magnification at 200 kv [25] as shown in Fig. 4.

Drug entrapment efficiency

The percentage drug entrapment was determined by the developed HPLC method. The Cur-NS were centrifuged at 11,000 rpm (REMI Cooling Centrifuge) for 15 min. After centrifuging, the supernatant was taken out and 1 ml of acetonitrile was added to the nanoparticle pellets, which were then sonicated for 5 min, to disrupt the structure of the particles and release curcumin. The amount of drug entrapped was then determined by using the developed HPLC method [24].

The percent entrapment efficiency was determined using the following equation:

$$\%DEE = \left[(\text{Curcumin encapsulated}/\text{Curcumin total}) \times 100\right]$$

In vitro drug release study

The in vitro drug release of the Cur-NS was studied by dialysis bag technique. Briefly, 1 ml of Cur -NS was taken in a dialysis bag (Hi-media Molwt molecular weight cut off between 12,000 and 14,000). The release was studied by suspending the bag in 200 ml of receptor medium (PBS 7.4 + 0.5 percent Tween 80) at 37 °C under continuous magnetic stirring using IKA HS 7. At regular intervals, 2 ml of samples were collected and replaced with fresh media. The drug concentrations in the collected

samples were then determined by the developed analytical HPLC method using the calibration equation $y = 18{,}005.5574x - 64979.1884$ $R^2 = 0.991$. [22]

Formulation and optimisation of Cur-NS loaded gel (Cur-NS-nanogel)

Preparation of plain gel

Carbopol 940 was dissolved in water and stirred continuously untill it dissolves completely. The polymeric solution was then cross-linked chemically by drop-wise addition of triethanolamineoleate with continous stirring at constant rate until a clear homogeneous gel was obtained [26].

Optimization and evaluation of the topical gel

The prepared gels were then optimized based on varying concentration (0.2–0.5%) of the polymer, the alkali (triethanolamine) and its effect on the physicochemical properties e.g. pH, Viscosity, Gel strength and Spreadability [27].

pH: pH of the gel was measured using a digital pH meter (μ pH system 361, Systonics). The pH meter was first calibrated with three standard buffers (pH 4, 7 and 9). After calibrating the apparatus, the pH of freshly prepared Carbopol 940 gels were measured by dissolving and equilibrating the required amount of gel in distilled water.

Viscosity: Viscosity of the prepared Gels were determined using Brookfield viscometer (DV-E Viscometer; Model No-LVDVE, USA) at 30 rpm/min using spindle No 64. The viscometer was calibrated using a standard solution of glycerine before all measurements.

Spreadability

Two sets of glass slides with uniform dimensions were used to test the spreadability of the produced gels. One of the slides was covered with the gel formulation. The gel was sandwiched between the two slides in an area that was occupied by a distance of 7.5 cm along with the slides when the other slide was positioned on top of the gel. The upper slides were given a 100-g weight to press the gel between them into a thin layer in a uniform manner. The excess gel that was sticking to the slides was scraped off after the weight was taken off. The two slides in place were securely fastened to a stand so that only upper slides could slip off freely under the force of weight tied on them. A 20 g weight was tied to the upper slide. The time taken for the upper slide to cover a distance of 7.5 cm and get separated from the lower slide under the force of the weight, was noted. The experiment was performed in triplicates and the meantime was taken for calculation [27, 28].

The following formula was used to determine spreadability:

$$S = m \times l/t$$

where, S = spreadability, m-weight tied to upper slides, l-length of the glass slide and t- time taken in sec.

Gel strength

The strength of the gel formulations was determined using a Texture Analyzer (Stable Micro System, FD/1–077). The "gelling strength test" or compression mode of the Texture Analyzer was selected, and the test speed was set to 1.0 mm/s. 50 points per second for the acquisition rate and 5 g for the trigger force were chosen. An aluminum probe of 7.6 cm diameter was used for all the samples. The immersion probe was inserted into the gel during the test at room temperature. Gel strength, expressed in grams, was used to determine the force necessary to penetrate the gel [28].

Preparation of Cur-NS-nanogel

The Nanogel was prepared by adding the Carbopol 940 in the Cur-NS followed by cross linking with triethanolamine. The nanosuspensions were then continuously stirred until homogenous nanogels were formed.

Evaluation of Cur-NS-nanogel

The nanogels were evaluated in terms of appearance, homogeneity, pH, viscosity, and spreadability as mentioned in the earlier sections.

Drug content in Cur-NS-nanogel

The drug content was measured by dissolving the measured amount of gel in acetonitrile. The dispersion obtained was filtered and analyzed at 425 nm using the developed HPLC method [29].

Drug loading efficiency (%) = (Experimental drug content/ Theoretical drug content) 100%

Stability studies

The accelerated stability studies were conducted in accordance to the ICH guidelines. The Cur-NS-Nanogel were kept at 4 °C, 25 °C and 40 °C and stability was observed for 30 days. The stability was observed in terms of change in color, appearance, pH, viscosity, and gel strength [30]

Ex vivo skin permeation study

Processing of rat skin

The albino Wistar rats were received from the animal house facility of Veterinary College, Khanapara. The animal study was conducted as per the CPCSEA guidelines after getting approval from the Institutional

Animal Ethical Committee (Ref no: GIPS/IAEC/M.PH/PRO/10/2022). Experimental animals were feed with standard commercial pellets with free access to water ad libitum and housed according to standard laboratory environment by maintaining a 12 h day and night cycle at normal room temperature of $25 \pm 1°C$ and 45–55% relative humidity. The rats (200–250 gm) were anesthetized using ketamine (30 mg/kg) [IP] anesthesia prior to excision of the skin and hairs were removed using hair clips. Excised skin were rinsed with 0.9% saline water [31].

Permeation study

The permeation through skin was studied using 20 ml modified franz diffusion cell assembly. The prepared rat skins were tied to the donor compartment such that the dermis faces the receiver compartment. The receptor compartment was filled with receptor media (PBS 7.4 + 0.5%Tween 80) and the donor compartment was loaded with 200 mg of Cur-NS Nanogel. The assembly was placed in a temperature controlled magnetic stirrer (IKA HS7) with temperature maintained at 37°C. Drug permeation study was conducted for 24 h under continuous magnetic stirring. 1 ml samples were withdrawn at regular time intervals from the receptor compartment and were analyzed using the developed HPLC method [32, 33].

Permeation kinetics analysis [33, 34]

The rate of drug permeation was determined using the Ficks Law of diffusion using the equation:

$$J = D.dc/dx$$

where J represents the rate at which a drug permeates a membrane, dc/dx represents a gradient in concentration, and D represents the diffusion coefficient of the drug. While steady state flux was computed using the following equation, lag time was calculated using the intercept of the slope.

$$J = KpCo$$

where Co represents the drug concentration and Kp represents the permeability coefficient.

$Kp = J/Co$ is the permeability coefficient that is obtained from the steady state flux.

Assessment of in vivo wound healing activity
Experimental animals

Unisex albino Wistar rats (220 ± 20 g) were used for assessing the cutaneous wound healing potential of the nanogel. Animal experimentation was approved by the Institution Animal Ethical Committee (IAEC) of GIPS, Guwahati (Approval number GIPS/IAEC/M.PH/PRO/10/2022).

Experimental animals were feed with standard commercial pellets with free access to water ad libitum and housed according to standard laboratory environment by maintaining a 12 h day and night cycle at normal room temperature of $25 \pm 1° C$ and 45–55% relative humidity [35].

Excision wound model

In the present study, the excision wound model was selected for evaluating the cutaneous wound healing potential of the curcumin nanogel [29]. To start with the model, all the 30 experimental rats were randomly assigned to five groups with six rats in each group ($n=6$) as listed below and were anesthetized using ketamine (30 mg/kg) [IP] anesthesia, before induction of the wound. The particular skin area of all the experimental rats was shaved 1 day prior to the experiment. Approximately 30 mm^2 of skin was removed from all the experimental animal groups except the normal group at a depth of 2 mm from a predetermined area of shaved skin to create the excision wound. After induction of the cutaneous wound, it was left undressed, exposed to an open environment and observed for any signs of infection. Normal saline solution was blotted onto the wound to achieve hemostasis. The wounded animals were housed separately in different cages.

- Group I (normal group): Animals receiving a normal diet and water ad libitum. Wounds were not induced in this group.
- Group II (No treatment group): Animals receiving a normal diet and water ad libitum + wound induction.
- Group III (Treatment with the plain gel): Animals receiving a normal diet and water ad libitum + wound induction + treatment with plain carbopol gel.
- Group IV (Standard Control): This group received normal diet and water ad libitum + wound induction + treatment with marketed turmeric cream (0.6% w/w equivalent curcumin).
- Group V: This group received a normal diet with water ad libitum + induction of excision wound + treatment with formulated (0.6% w/w equivalent curcumin) Cur-NS-Nanogel.

During the treatment period, the area of the wound was measured on 0th, 5th, 10th, 15th, and 21st day using the Android software, Imito Measure (https://imito.io/en) [18] and the percentage wound contraction was calculated using the formula given below [36].

$$\% \text{ Wound Contraction} = [(\text{Wound Area in Day 0} - \text{Wound Area on day } n) / \text{Wound Area on day 0}] \times 100$$

On the 21st day of operation, a fraction of the excised tissues from each group were processed for histopathological examination. For conducting the

histopathological analysis, a 10% buffered formalin block was used and blocked with paraffin. Further the tissues were sliced into 5 mm thickness and stained with hematoxylin and eosin dye (H-E dye) followed by photography and examination of the tissues [37]. The results are shown in Figs. 5 and 6.

Acute anti inflammatory activity

Prior to the experiment, animals were allowed unlimited access to water while fasting for 24 h. Except for normal control (group I), all animal groups received 0.05 ml of a 1% suspension of carrageenan in saline on the day of the experiment. One hour prior to each experiment, the carrageenan solution was produced and administered to the rat's right hind paw's plantar side. With the examined sample, Groups III to IV were processed and topically applied to the plantar surface of the hind paw by rubbing 50 times, gently with the index finger. The study's standard reference medication was 0.5% piroxicam gel. One hour before the carrageenan injection, medications were administered. Using a plethysmometer, paw volume was measured immediately following the injection of carrageenan and at intervals of 1, 2, 3, and 4 h [32, 38]. The results are shown in Fig. 7.

Statistical analysis

The standard error of the mean (SEM) was used to express all values of the experimental data. Analysis of variance (ANOVA) was performed for the evaluation of the wound area from postoperative day 0 to 21 using a two-way ANOVA statistical procedure, followed by Bonferroni's post-test for multiple comparisons between groups. All statistical analyses were performed using GraphPad Prism 5.0 software (GraphPad Software, Inc., La Jolla, CA). A difference in the mean values with $p < 0.05$ was considered to be statistically significant.

Results

Physical evaluations and phytochemical studies of the LKD successive extracts

Table 1 reports the physical characteristics and yield percentages of the successive LKD extracts. In the present investigation, the quantification of total phenolic and tannin content as demonstrated in Table 1 depicted that the LKDCH extract (2.16 ± 0.62 mg GAE/g of dry weight extract) showed the presence of maximum quantity of phenolics and tannins followed by LKDME, LKDEA and LKDHE. The results of phytochemical screening are shown in Table 2. The HPTLC fingerprint analysis of LKDCH when compared to standard reference curcumin showed a prominent and dense bands
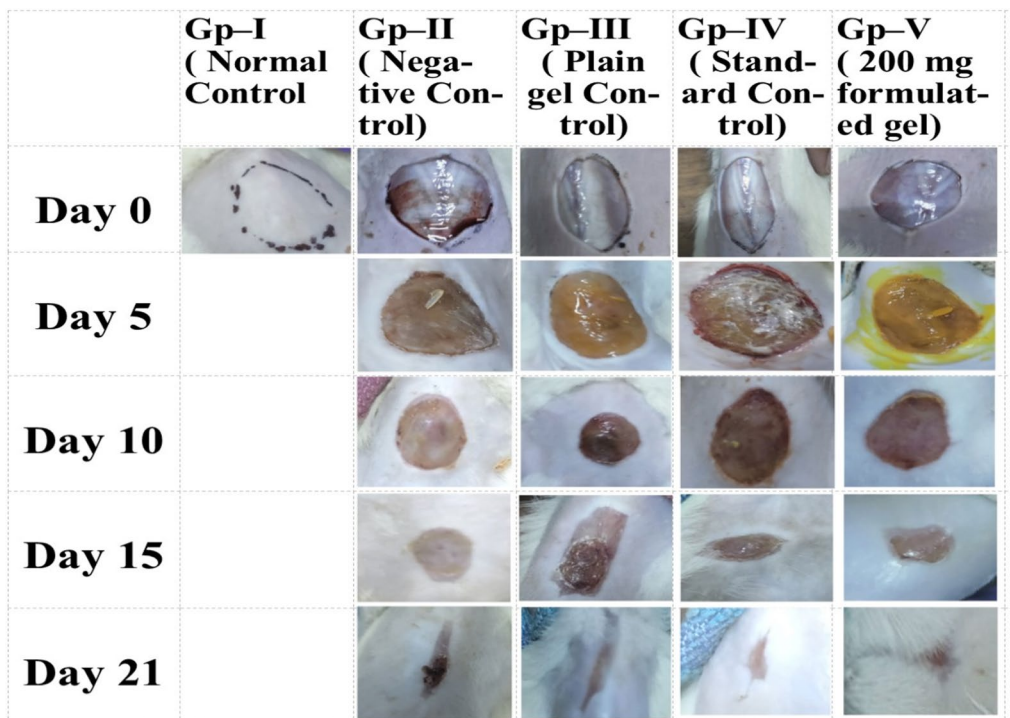

Fig. 5 Wound structural changes and healing effects from day 0 to day 21 after treating with tested samples
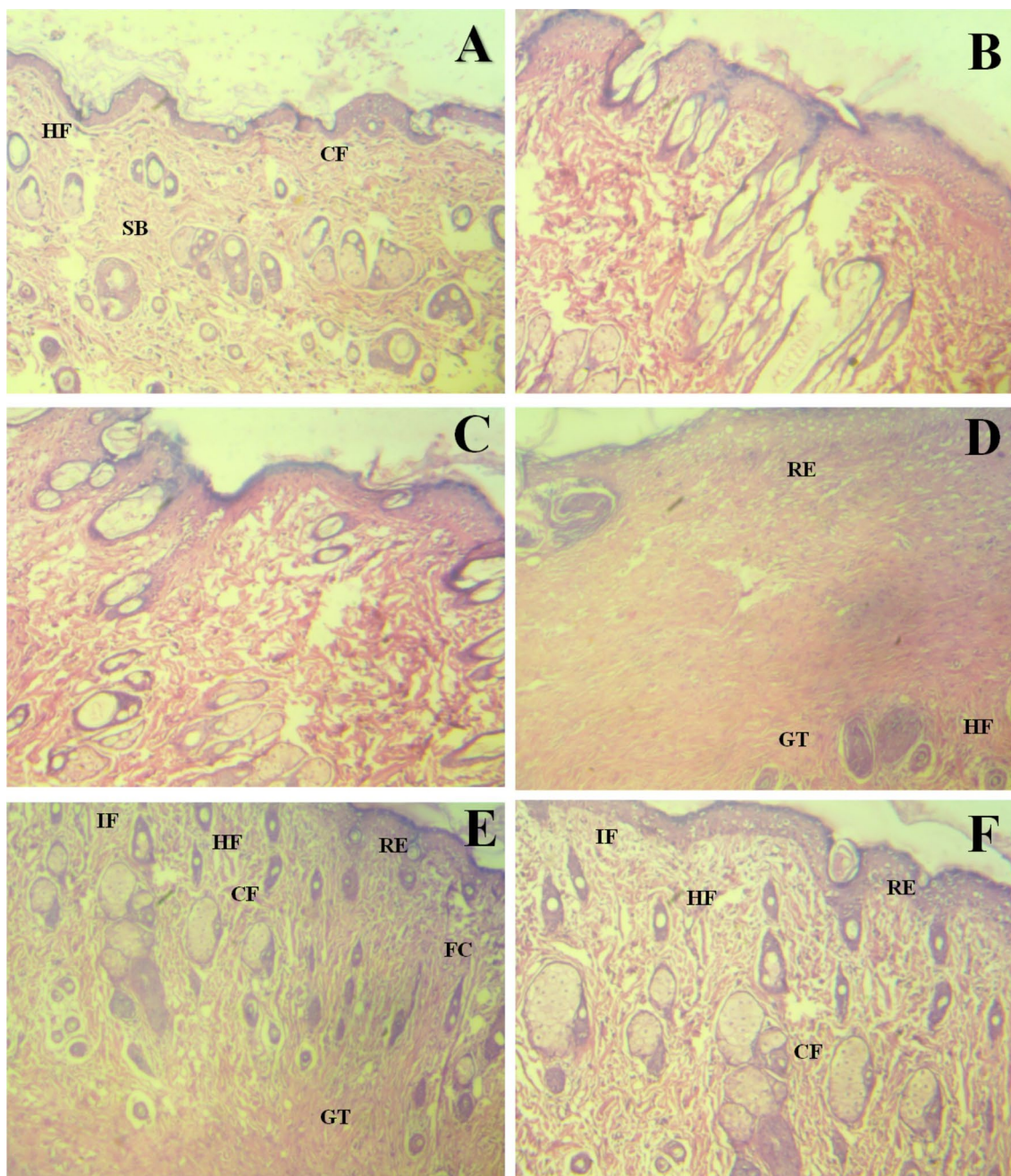
Fig. 6 Histopathologicalsection analysis of the rat skin tissues obtained from the 21st-day excision wound model: **A**: Normal control group; **B**: Negative control group; **C**: Group treated with plain carbopol gel; **D**: Group treated with marketed turmeric cream (0.6% equivalent curcumin); **E** and **F**: Group treated with Cur-NS-Nanogel(0.6% equivalent curcumin) [CF: Collagen fibers, FC: Fibroblast cells, HF: Hair follicles, IF: Inflammatory cells, RE: re-epithelization, GT: Granulation tissues, SB: Sebaceous gland]

of curcumin and its two analogues viz bisdesmethoxy-curcumin (BDMC) and demethoxycurcumin (DMC) having Rf value at 0.81, 0.65 and 0.53 respectively. Gas chromatography analysis revealed that all the LKD extracts were found to be devoid of any residual solvent (Additional file 1: Fig. S1).
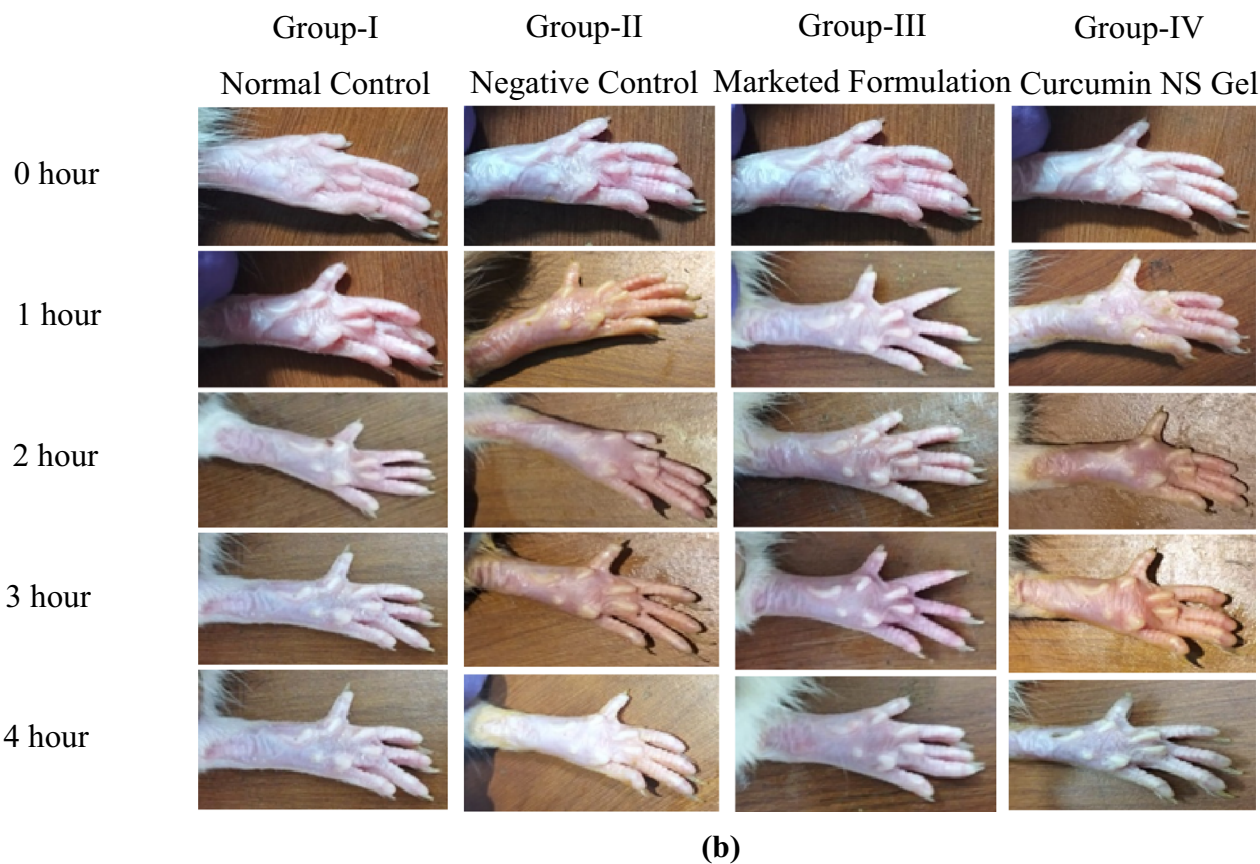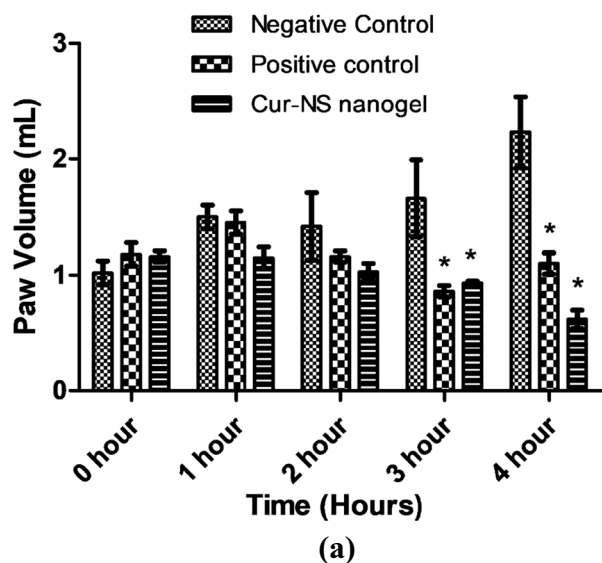
Fig. 7 **a** Effects of Cur-NS nanogel in paw volume in rats at different time intervals, **b** *In vivo* anti inflammatory activity of Cur-NS nanogel in rats

In vitro antioxidant activity

DPPH radical scavenging activity of LKD successive extracts is shown in Fig. 1. Data demonstrated that LKDHE, LKDEA, and LKDME extracts showed significant ($^*p < 0.05$) difference when compared to the positive control (STD-CUR) revealing their less antioxidant efficacy. However, LKDCH showed statistically non-significant ($^{ns}p < 0.05$) when compared to STD-CUR,

Table 1 Physical properties, % yield and total phenolic and tannin content of the successive LKD extracts

Solvent	Nature & pH	Colour and odour	Solubility	Percentage of yield (% w/w)	Total phenolic content (mg TAE/g extract)	Total Tannin content (mg TAE/g extract)
LKDHE	Semisolid pH-6.6	Yellow	Highly soluble in hexane, chloroform and sparingly soluble in methanol	3.3%	0.42 ± 0.10	0.07 ± 0.11
LKDCH	Amorphous pH-7.8	Yellow crimson red	Highly soluble in chloroform and moderately soluble in methanol	7.9%	2.16 ± 0.62	1.91 ± 0.18
LKDEA	Amorphous pH-7.74	Light yellow	Highly soluble in ethyl acetate and methanol	1.8%	0.85 ± 0.22	0.49 ± 0.14
LKDME	Amorphous pH-7.9	Brown	Soluble in methanol	3.4%	0.98 ± 0.19	0.55 ± 0.12

Table 2 Preliminary phytochemical screening of various successive extracts of LKD

Phytoconstituents	LKDHE	LKDCH	LKDEA	LKDME
Alkaloids	−	−	−	−
Glycosides	−	+	+	+
Flavonoids	−	+	+	−
Steroidal/triterpenes	+	+	+	+
Phenolic & tannins	−	+	+	+
Saponins	−	−	−	−
Mucilages	−	−	−	−
Proteins	−	−	−	+
Amino Acids	−	−	−	−
Sugars	−	−	−	+
Fixed oil	+	+	−	−

indicating that it has the ability to scavenge the DPPH radical which is comparable to the standard.

Isolation and structural elucidation of curcumin from LKD

Column chromatography of the LKDCH yields 105 fractions. The existence of curcuminoid components was shown by fraction numbers 50–76 as depicted on the TLC chromatogram. Fraction 50–55 demonstrated the highest purity based on the TLC profile as indicated by the presence of a significant dense area of curcumin with modest amounts of BDMC and DMC. Further, this fraction (50–55) was purified by re-crystallization in ethanol, as indicated in the literature [39], thus yielding a yellowish crystals of curcumin. The purified curcumin was lyophilized and characterized by NMR, FT-IR, Mass and UV–Visible spectrophotometer. The melting point of the compound was observed at 181 °C and the UV–visible spectrum with λ_{max} was recorded at 425 nm. IR bands (υ cm^{-1}) showed the presence of prominent functional groups of curcumin at 3653 (–OH), 2979 (C–H), 1625 (C=C), 1264 (C–O–C), 1026 (C-O-H). ^{1}HNMR spectrum (400 MHz, DMSO-d$_6$) produces prominent proton peaks (δ ppm) at 3.837 (s, 6H, OCH$_3$), 6.056 [s, 1H, C(OH)=CH], 6.777 (d, 2H, 2,6-H), 6.833 (d, 2H), 7.160 (d, 2H), 7.325 (s, 2H), 7.567 (d, 2H, 1,7–H), 9.667 (br s, 2H, phenolic –OH). Chemical shift with δ value at 3.837 depicted a singlet peak which corresponds to the existing of two methoxy groups; whereas, a sharp δ value at 9.667 represent the presence of phenolic hydroxy group. The two aromatic proton signals at δ value region of 6.833 and 7.160 each of them integrated for four protons diagnostic for two identical para-substituted benzene rings. ^{13}C NMR spectrum (125 MHz, DMSO) represents distinct carbon peaks (δ ppm) at 55.60, 100.79, 111.29, 115.64, 121.00, 123.02, 126.26, 140.63, 147.91, 149.27, 183.12. ^{13}C NMR chemical shift with δ value at 55.60 clearly signify the carbon atom corresponding to methoxy group; whereas, δ value at 183.12 depicted the carbon atom corresponding to enol and keto group. Furthermore, the mass spectra (TOF–MS-ES$^+$) depicted that the base peak at *m/z* 177.056 and a molecular ion peak [M+H]$^+$ at 369.135 was detected. All these analytical spectroscopic features are in line with the data reported in the literature thus signifying the identity of curcumin isolated from Lakadong rhizome [17, 40, 41]. The results are shown in Fig. 1.

Formulation of Curcumin loaded nanosuspension

Homogenous nanosuspensions were obtained by the precipitation-sonication method. The precipitation method of nanosuspensions preparation is instantaneous, straightforward and easy [42].

Characterization of curcumin NS

Particle size distribution and zeta potential

The particle sizes of the Cur-NS were found to be in the range of 150 ± 50 nm and PDI 0.2 ± 0.1, indicating suitable size and distribution. From the study, the Zeta Potential of the formulations was found to be -2.92 ± 0.2 mV.

Optimization of the Cur-NS

The nanosuspensions were optimized by using drug concentration, ratio of organic phase to aqueous phase, Polymer (PLGA) concentration, and stabilizer (Poly vinyl alcohol) concentration as the variables. The effects of these independent variables on the dependent variables (particle size, polydispersity Index and drug release) were observed to get the optimized formulation. From the study saturation drug concentration of 60 mg/ml, solvent: antisolvent (S:NS) ratio of 1:20, PLGA concentration at 0.25% and PVA concentration of 0.6% were considered as optimized variable conditions as shown in Table 3. F3, which was the optimized NS, was found to have particle size of 157.1 ± 2.4 and polydispersity index 0.132 ± 0.052.

Transmission electron microscopy (TEM)

The morphology and size of the formulations were observed by TEM studies. The nanoparticles were observed to be uniform in size within the range of 100–200 nm and spherical in shape.

Entrapment efficiency of Cur-NS

The entrapment efficiency was determined by the HPLC method. The entrapment efficiency of Cur-NS was found to be $98.52\% \pm 0.2$ which can be considered sufficient.

In vitro drug release

In vitro release behavior of Curcumin from the optimized Cur-NS was observed for 24 h. A sustained drug release rate was observed with almost 80% drug being released in initial 4 h indicating an initial burst release followed by sustained release upto to $90.0 \pm 1.6\%$ in 24 h.

Preparation of Cur-NS based topical gel

Homogenous nanogels were obtained by adding the Carbopol as the gelling agent in the optimized Cur-NS, followed by cross linking by addition of triethanolamine as the alkali.

Optimization and evaluation of the topical gel

Evaluation of the Cur-nanogels

The Cur-Nanogel was optimized by observing the effect of varying concentration (0.2–0.5%) of the Carbopol and alkali (triethanolamine) and its effect on the physicochemical properties e.g. pH, Viscosity, Gel strength and Spreadability. The pH, viscosity, gel strength and spreadability of the prepared Cur-Nanogels were found to be optimum at Carbopol Concentration of 0.3%. The optimized Cur-Nanogel was found to be smooth, translucent, clear, homogenous with good spreadability and consistency. The gels showed good consistency with Viscosity of $20,480 \pm 456$ cp, which was a desired consistency for patient compatible topical application. The spreadability was found to be 20.0 ± 1.6 g/cm^2. The gels showed good gel strength of 9.0 ± 0.4 g and showed slightly acidic pH at 6.50 ± 0.3 which is safe for topical application as shown in Table 3.

Drug loading in Cur-nanogel

The drug loading efficiency in the prepared Cur-Nanogel was determined by the HPLC method. Sufficient drug loading of $61.2 \pm 4.5\%$ was obtained by the method used for preparation of nanogel in the optimized Cur-NS.

Stability studies

Stability studies of developed formulation were performed according to ICH guidelines for 30 days. From the study it was observed that the optimized formulation exhibited good stability behavior in terms of pH, physical appearance, viscosity, spreadability and drug content as shown in Table 4. No change in properties of the gel is observed for the formulations stored at room temperature, 4 °C and 40 °C.

Ex vivo skin permeation study

From the ex vivo skin permeation Study using rat skin, Cur-NS-nanogel showed a much controlled permeation

Table 3 Formulation table for optimized Curcumin Nanosuspension (Cur-NS)

Formulation	PVA %	PLGA mg	Drug mg/ml	S:NS	Particle Size nm ± SD	PDI ± SD	Drug Release in 24 h % ± SD
F3	0.5	30	60	1:20	157.1 ± 4.6	0.130 ± 0.014	90 ± 1.6

Table 4 Evaluation of Optimized Cur- NS Loaded Nanogel

Formulation	Concentration of Carbopol %	Physical Appearance	Viscosity cp ± SD	pH ± SD	Spreadabilty g/cm^2 ± SD	Gel Strength g ± SD
NG3	0.3	Smooth and homogeneous	20,480 ± 590	6.5 ± 0.3	20.00 ± 2.4	9.00 ± 0.6

Table 5 Stability studies results of Cur-NS Nanogel

Parameter	Day 0			Day 30		
	4 °C	RT	40 °C	4 °C	RT	40 °C
Viscosity Cp ± SD	23,200 ± 600	23,200 ± 600	23,200 ± 600	23,000 ± 400	25,200 ± 300	19,600 ± 700
pH ± SD	6.5 ± 0.3	6.5 ± 0.3	6.5 ± 0.3	6.6 ± 0.2	6.6 ± 0.3	6.2 ± 0.5
Gel Strength g ± SD	9.2 ± 0.4	9.2 ± 0.4	9.2 ± 0.4	8.5 ± 0.5	8.5 ± 0.2	5.5 ± 0.6

with steady state flux of 21.28 ± 0.23 µg/cm^2/hr in 24 h in comparison to Plain Carbopol gel which showed higher steady state flux of 36.38 ± 0.23 µg/cm^2/hr. The permeation coefficients were similarly found to be $2.031 \pm 0.0064 (\times 10^3$ cm/min) and 3.6 ± 0.0064 ($\times 10^3$ cm/min) in Cur-NS-Nanogel and Plain Carbopol Gel respectively (Table 5).

Cutaneous wound healing potential of Cur-Nanogel

In the current study, nanoformulation of curcumin was found effective in healing cutaneous wounds. Figure 5 represents the morphological and structural changes of the wounds from day 0 to day 21 after being treated with the curcumin nanoformulation. Animals treated with simple carbopol gel showed no significant difference ($p < 0.05$) in the wound contraction area on comparision to the negative control group (untreated group). However, topical treatment of the animal groups with commercially available turmeric cream (0.6% w/w equivalent curcumin) and formulated CUR-NS nanogel of equivalent percentage of curcumin on day 5, 10, 15 and 20 showed a significant ($^*p < 0.05$) reduction in the wound contraction area when compared to the untreated group. The percentage wound contraction (%) and epithelialization period concerning plain gel, standard control, and that of the tested CUR-NS nanogel is respectively shown in Table 6. The nanogel resulted in better healing of the open wound in comparison to marketed turmeric cream with equivalent curcumin. The percentage wound contraction was found to be significantly higher in the prepared nanogel in comparison to the marketed

cream. Results from the histopathological analysis also supported our study. Tissues excised from the normal control group revealed normal hair follicles (HF), collagen fibers (CF) with well defined-outer epidermis and well-organized epithelial cells (EC) as depicted in Fig. 6A. While tissues excised from the negative control group and the plain gel treated group exhibited remarking deterioration of the epithelial cells (EC) and the epidermis (ED), along with damaged collagen fibers (Fig. 6B and C). However, marketed turmeric cream applied on the animal group exhibited sufficient healing ability represented by re-epithelialization and regeneration (Fig. 6D). The experimental groups receiving the tested CUR-Nanogel represented excellent cutaneous wound healing capability.

Acute anti-inflammatory activity

Figure 7a and b demonstrated the anti-inflammatory effects of the formulated Cur-NS nanogel in the carrageenan-induced paw edema model in experimental rats. The result depicted that subcutaneous injection of carrageenan at 0th, 1st and 2nd hour showed no discernible ($p > 0.05$) changes in the paw volume in both untreated (negative control) and treated rats (Cur-NS nanogel and positive control). Topical intervention with Cur-NS nanogel (0.6%) at 3rd and 4th hour when compared to negative control rats demonstrate a significant ($^*p < 0.05$) reduction in the paw volume by 43.97% and 72.19% respectively. Similar but lesser effect was seen with topical intervention applied with marketed curcumin formulation (positive control), where the paw volume also

Table 6 Wound Healing study results in rats from day 0 to day 21

Experimental group	Wound area (cm^2) and percentage of wound contraction					
	Day 0	Day 5	Day 10	Day 15	Day 21	% wound contraction
Gp-I (Normal control)	–	–	–	–	–	–
Gp-II (Negative control)	3.37 ± 0.45	3.19 ± 0.45	2.83 ± 0.44	1.42 ± 0.55	0.33 ± 0.09	90.23%
Gp-III (Plain Gel control)	3.2 ± 0.29	2.7 ± 0.48	2.05 ± 0.30	0.79 ± 0.39	0.41 ± 0.15	87.18%
Gp-IV (Marketed Gel)	3.37 ± 0.28	3.5 ± 0.25	2.66 ± 0.27	0.95 ± 0.37	0.19 ± 0.08	94.72%
Gp-V (Formulated 200 mg gel)	3.25 ± 0.27	2.91 ± 0.27	1.64 ± 0.34	0.50 ± 0.29	0.14 ± 0.06	95.69%

showed significant reduction ($^*p < 0.05$) at 3rd (48.19%) and 4th hour (50.67%).

Discussion

Curcuminoids, which are abundant in turmeric, have several biological functions. Curcumin, in particular, has been proven to have a wide spectrum of therapeutic effects in both pre-clinical and clinical studies. Curcumin analogues' biological capabilities have recently been documented, with demethoxycurucmin (DMC) being shown to be very effective in suppressing MCF-7 cells and bisdemethoxycurcumin (BDMC) having the capacity to modify MDR-1 gene expression. Among all the known curcuminoids, except curcumin, both DMC and BDMC are not commercially available [43]. As a result, it is essential to isolate curcuminoids at a high purity in order to study their biological properties. The current study investigated the process of isolation and purification of curcumin from Meghalaya Lakadong turmeric and formulation of novel nanogel for evaluation of its wound healing and anti-inflammatory activities in experimental animals. Our reports demonstrated that among the LKD successive extracts, the yield percentage was found to be highest with that of LKDCH. The density of the color change during phytochemical screening of the LKDCH indicated the presence of a significant amount of phenolics, tannins, terpenes, and steroids. Our findings are consistent with those of previous research [44–46], where turmeric samples gathered from various parts of the world showed comparable and similar phytochemical profile. The total residual solvent present in all the successive extracts were found to very minimum as evident from the results of Gas Chromatography studies, which depicted that the extract is free from harmful residual solvents used during extraction process. Literature demonstrated that the presence of residual solvent beyond the safety limits may be associated with carcinogenicity, neurotoxicity, teratogenicity and may other toxic consequences in finished herbal medicinal products [47]. Based on the quantitative estimation, it was observed that total phenolic and tannin content was found to be highest with LKDCH extract (2.16 ± 0.62 mg GAE/g of dry weight extract) as compared to other successive extracts. The high phenolic content of turmeric may be attributed to the presence of curcuminoids and other phenolic components [48]. Research reported that the total phenolic content present in ordinary turmeric (*Curcuma* longa) was 1.03 mg GAE/gm dry weight extract [49]. Based on these findings, it is evident that Lakadong turmeric grown in Meghalaya has a higher phenolic content (two-fold) than ordinary turmeric, which is in agreement with the literature which reports that LKD turmeric contains high levels of phenolic curcuminoids

[50]. As evidenced by our HPTLC fingerprinting analysis, the LKDCH extract showed higher levels of curcumin in comparison to the reference curcumin, while BDMC and DMC were significantly less dense. This marks the initial instance of curcumin isolation from Lakadong turmeric, and the spectral data align precisely with the previously documented curcumin spectra in existing literature [17, 39–41, 43].

Scavenging of the stable free radical (DPPH) is regarded as a reliable test for assessing antioxidant scavenging activity of a substance [51]. Plant extracts containing polyphenol components have antioxidant action due to their ability to donate hydrogen atoms or electrons and trap free radicals [52]. According to research, the phenolic OH group or the CH_2 group of the β-diketone moiety can both contribute to curcumin's ability to neutralize and scavenge free radicals [53]. In the current study, it was found that the LKDCH extract consists of a significant amount of phenolic and tannin contents, with curcumin as its main constituent. Therefore, the presence of curcuminoids, which have substantial antioxidant activity, may be responsible for the DPPH radical scavenging activity of the LKDCH extract.

Homogenous nanosuspensions were obtained by the precipitation-sonication method. The precipitation method of nanosuspensions preparation is instantaneous, straightforward and easy [42]. The high drug saturation concentration and the rapid solvent injection into the antisolvent results in such precipitation into nanoparticles [22]. The precipitation followed with sonication results in better homogeneity in the precipitated nanoparticles [54]. PLGA based nanosuspension were prepared since they provide a number of benefits for drug administration via the skin, such as non-toxicity and biodegradability, and since hydrolysis results in the generation of water and carbon dioxide as well as effective drug entrapment [55, 56]. Additionally, PLGA-based nanoparticles have the benefits of controlled and sustained release and may lessen the irritation associated with direct contact of drug with skin [55].

The particle sizes of the Cur-NS were found to be in the range of 150 ± 50 nm and PDI 0.2 ± 0.1, indicating suitable size and distribution. This size range and the homogeneity are because of the method of preparation by precipitation followed by sonication. This decreased size might result in increased surface area which may result in the increased saturation solubility and release of curcumin [54]. From the study, the Zeta Potential of the formulations were found to negative that might be due to the surfactant or due to the terminal carboxylic groups. The reduced surface charge reflects better surface coverage due to the use of non ionic surfactant which results in steric stabilization. PVA was used as a steric stabilizer

since steric stabilization has several advantages over electrostatic stabilization as the nanoparticles have good redispersibility; dispersion medium elimination is possible even in high concentration of nanocrystals and less salting out [57]. The nanosuspensions were optimized by using drug concentration, ratio of organic phase to aqueous phase, Polymer (PLGA) concentration, and stabilizer (Poly vinyl alcohol) concentration as the variables. The effects of these independent variables on the dependent variables (particle size, polydispersity Index and drug release) were observed to get the optimized formulation. From the study saturation drug concentration of 60 mg/ml, solvent: antisolvent (S:NS) ratio of 1:20, PLGA concentration at 0.25% and PVA concentration of 0.6% were considered as optimized variable conditions as shown in Table 3. It was observed that with increasing drug concentration the size and dispersity decreases indicating the impact of supersaturation in the nanoprecipitation. However at higher concentration, above 60 mg/ml the size increases. Similarly, it was observed that the particle size and dispersion decrease with increase in S: NS ratio from 1:10 to 1:20. Similar behaviors were reported in previous works on nanosuspension by this method [22, 58]. The concentration of PLGA and stabilizer didn't show any direct correlation with the size distribution of the precipitated nanoparticles.The morphology and size of the formulations were observed by TEM studies. The nanoparticles were observed to be uniform in size in correlation to the zetasizer observations and were spherical in shape.

The entrapment efficiency was determined by the HPLC method. The entrapment efficiency of Cur-NS was found to be sufficient (98.52% ± 0.2). The high entrapment is because of the precipitation method of preparation of nanosuspensions. In this method technique the drug which is hydrophobic in nature is soluble in organic solvent but is very slightly soluble in water. Nanoparticles with high entrapment efficiency were obtained as a result of reduced or very negligible drug leakage towards the outer medium [59, 60]. In vitro release behavior of Curcumin from the optimized Cur-NS was observed for 24 h. A sustained drug release rate was observed in initial 4 h indicating an initial burst release followed by sustained release upto 24 h. The improved drug release may be due to the increased surface area of the nanoprecipitation drug particles. The presence of PLGA might be responsible for the controlled and sustained release behavior observed [55].

Homogenous nanogels were obtained by adding the Carbopol as the gelling agent in the optimized Cur-NS, followed by cross linking by addition of triethanolamine as the alkali. The Cur-Nanogel was optimized by observing the effect of varying concentration of the Carbopol and alkali (triethanolamine) and the pH, viscosity, gel strength and spreadability of the prepared Cur-Nanogels were found to be optimum at Carbopol Concentration of 0.3%. The optimized Cur-Nanogel was found to be smooth, translucent, clear, homogenous with good spreadability and consistency. The obtained properties of prepared gel were found suitable, safe for compatible topical application, particularly in wound healing. The obtained properties might have resulted in non-adhesiveness, exudate absorption, retention of moisture, and gas permeability which were ideal for wound healing application [12].

Sufficient drug loading (61.2 ± 4.5%) was obtained by the method used for preparation of nanogel in the optimized Cur-NS. The high drug loading might be due to the method of preparation of gel by simultaneous addition method. From the ex vivo skin permeation Study using rat skin, Cur-NS-nanogel showed a much controlled permeation with higher steady state flux in comparison to Plain Carbopol gel. Similar results were obtained for the partition coefficients. This controlled permeation may be due to the presence of PLGA in the nanogel and may result in better anti-inflammatory and wound healing activity with reduced nanotoxicity on application. Stability studies of developed formulation showed that optimized formulation exhibited good stability behavior in terms of pH, physical appearance, viscosity, spreadability and drug content in different conditions.

Different stages of wound healing like inflammation, proliferation and regeneration often overlap with each other and are difficult to differentiate resulting in enhanced qualitative and quantitative aspects of each stage which might hasten the healing process with reduced side effects [61]. In the current study, nanoformulation of curcumin was found effective in healing cutaneous wounds. The experimental groups receiving the tested CUR-Nanogel represented excellent wound healing capability with re-epithelialization, regeneration and reformation of fibroblast cells (FC), granulation tissues (GT), hair follicles (HF), collagen fibers (CF) and inflammatory cells (IC) (Fig. 6E, F). Fibroblast cells (FC) aid cell migration and proliferation by the production of primary extracellular matrix, including fibronectin, hexosamine, hexuronic acid in the wound bed and is primarily responsible for collagen formation [36, 62, 63]. These fibroblast cells are matured into fibrocytes with higher ability of collagen formation after discharging to the wound sites [64]. Moreover, the inflammatory cells intensify the inflammatory response with the release of certain chemotoxic agents to disinfect the wound area [61, 65]. However, a cumulative aggregation and cell hyperactivation in the wound area might result in pus formation

Sarma *et al. Future Journal of Pharmaceutical Sciences* (2023) 9:85

Page 18 of 21

in the wound site, leading to amputation and loss of tissues, and thus affecting the healing process. Again, in the infection site, the formation of pus is aided by the formation of free radicals which can be scavenged by the use of antioxidants [66, 67]. The antioxidants in the curcumin would thus assist in complete healing of the wounds by scavenging the free radicals and pus within the infected area. Hence, in the current study, Cur-Nanogel demonstrated excellent cutaneous wound healing potential as compared to the marketed turmeric extract cream.

λ-Carrageenan, a complex polysaccharide, is a routine inflammatory inducer that causes rapid inflammatory reactions, including increased pain sensitivity and skin redness. This is due to the activation of several pro-inflammatory pathways including histamine, bradykinin, tachykinins, cyclooxygenase, and reactive oxygen species (ROS). These mechanisms all contribute to the development of enlarged paws produced by fluid leaking into injection sites. This phenomenon is a useful metric for assessing anti-inflammatory medicines and their biological mechanisms, particularly their influence on the activation of pro-inflammatory cytokines and chemokines [68]. Carrageenan-induced paw edema is a popular experimental paradigm for evaluating anti-inflammatory drugs due to its dependability and precision in producing findings [69]. Turmeric and its bioactive constituent 'curcumin' are well known for their anti-inflammatory effects with well defined mechanism by regulating various inflammatory signaling pathways and inhibiting the production of proinflammatory mediators [70]. Many researches have demonstrated that curumin alone or its pharmaceutical formulation showed a dramatical inhibition on inflammation of the paw edema produced by carrageenan [71]. Our result is in accordance with the data reported in the literature, depicting that PLGA-based curcumin nanosuspension loaded in carbopol gel revealed significant anti-inflammatory effects in experimental rats. This increased anti-inflammatory activity in the Cur-NS Nanogel may be due to the more controlled permeation of the drug because of the presence of PLGA in the nanogel that may have resulted in better anti-inflammatory and wound healing activity [72]. Such controlled permeation of nanoformulation may be essential for ensuring reduced nanotoxicity on application. The observed behavior may also be due to the quality and purity of isolated curcumin from LKDCH, used in the Cur-NS nanogel in comparison to the marketed curcumin formulation.

Conclusion

From the study it may be concluded that the LKD show high curcumin content with its chloroform extract showing higher yield of curcumin of high purity with significant antioxidant effects. Homogenous curcumin nanosuspensions could be obtained by nanoprecipitation method using PLGA with suitable size distribution and physicochemical properties. LKD curcumin nanosuspensions could be converted into to stable Carbopol based nanogel with safe and controlled skin permeability with reduced nanotoxicity. This controlled and sufficient skin permeability of Cur-NS nanogel might result in significant and promising wound healing and anti-inflammatory activity in experimental rats. Hence LKD turmeric may be explored more for its high and pure curcumin content and suitable nanoformulations in the form of nanogel may be designed for better clinical applications of curcumin for inflammation and cutaneous wound healing.

Abbreviations

PLGA	Poly (lactic-co-glycolic acid
NS	Nanosuspension
SC	Stratum corneum
PVA	Poly Vinyl alcohol
LKD	Lakadong
LKDHE	Lakadong Hexane Extract
LKDCH	Lakadong Chloroform Extract
LKDEA	Lakadong Ethyl Acetate Extract
LKDME	Lakadong Methanol Extract
TLC	Thin Layer Chromatography
TP	Total phenolics
TSP	Total simple phenolics
TC	Tannin content (TC)
HPTLC	High Performance Thin Layer Chromatography
MeOH	Methanol
CHCL3	Chloroform
FT-IR	Fourier Transform InfraRed
HPLC	High Performance Liquid Chromatography
NMR	Nuclear Magnetic Resonance
DSC	Differential Scanning calorimetry
DMSO	Dimethylsulfoxide
TMS	Tetramethylsilane
ppm	Parts per million
DPPH	1, 1 Diphenyl-2-picrylhydrazyl
HRBC	Percentage stabilization of human red blood cell
PDI	Polydispersity index
DLS	Dynamic light scattering
TEM	Transmission electron microscopy
ICH	International Council for Harmonisation
CCSEA	Committee for Control and Supervision of Experiments on Animals
IAEC	Institutional animal ethical Committee
SEM	Standard error of mean
ANOVA	Analysis of variance
BDMC	Bisdesmethoxycurcumin
DMC	Demethoxycurcumin

Supplementary Information

The online version contains supplementary material available at https://doi.org/10.1186/s43094-023-00534-9.

Additional file 1. GC chromatogram of residual solvents of hexane, chloroform,ethyl aceate and methanol extracts.

Additional file 2. Standard curcumin datasheet.

Author contributions

SKS: Methodology, Investigation, Writing-Original Draft. UD: Methodology, Investigation of formulation part. AB: Wound Healing work, Formal analysis, review & editing, SK: Methodology, Investigation (extraction and isolation), SB: All animal experimentations, histopathology and evaluation, HS: Instrumental analysis and evaluation, DL: Supervision, conceptualization, Writing, proof checking, revision & editing (Extraction & isolation Part), BPS: Supervision, conceptualization, Writing, proof checking, revision & editing (Formulation and Evaluation part). All author read and approved the final manuscript.

Availability of data and materials

The datasets generated during and/or analyzed during the current study are available from the corresponding author on reasonable request.

Declarations

Ethics approval and consent to participate

The animal work was performed with approval from IAEC approval no: GIPS/IAEC/M.PH/PRO/10/2022 under CSCEA guidelines. No human subjects were involved in the work.

Consent for publication

No personal data of individuals was used in the current study.

Competing interests

The authors have no relevant financial or non-financial interests to disclose.

Author details

[1]GIPS, Assam Science and Technology University, Guwahati, India. [2]Advanced Drug Delivery Laboratory, School of Pharmaceutical Sciences, Girijananda Chowdhury University, Guwahati, Assam 781017, India. [3]Pharmacology and Toxicology Laboratory, School of Pharmaceutical Sciences, Girijananda Chowdhury University, Guwahati, India. [4]Sophisticated Analytical Instrumentation Facility, Girijananda Chowdhury University, Guwahati, India. [5]Phytochemical Research Laboratory, School of Pharmaceutical Sciences, Girijananda Chowdhury University, Guwahati 781017, India.

References

1. M Manju TG Sherin KN Rajasekharan 2009 Curcumin analogue inhibits lipid peroxidation in a freshwater teleost, Anabas testudineus (Bloch)—an in vitro and in vivo study Fish Physiol Biochem 35 413 420 https://doi.org/10.1007/s10695-008-9266-6
2. H Hayakawa Y Minaniya K Ito Y Yamamoto T Fukuda 2011 Difference of curcumin content in *Curcuma longa* L. (Zingiberaceae) caused by hybridization with other curcuma species Am J Plant Sci 2 2 111 119 https://doi.org/10.4236/ajps.2011.22013
3. PB Kanjilal R Kotoky RS Singh 2002 Morphological and chemical parameter of certain cultivars of chilli, ginger and turmeric grown in Meghalaya Adv Plant Sci 15 1 225 229
4. R Chandra DS Yadav N Rai P Sarma 2005 Megha turmeric 1: a new turmeric for Meghalaya Indian Horticult 50 2 18
5. P Daimei Y Kumar N Sheikh NL Pfoze S Paduna 2012 The finest Lakadong variety of turmeric from the Jaintia Hills of Meghalaya India Pleione 6 1 141 148
6. S Tripathy DK Verma M Thakur AR Patel PP Srivastav S Singh AK Gupta ML Chávez-González CN Aguilar N Chakravorty HK Verma GL Utama 2021 Curcumin extraction, isolation, quantification and its application in functional foods: a review with a focus on immune enhancement activities and COVID-19 Front Nutr 8 747956 https://doi.org/10.3389/fnut.2021.747956
7. KY Yang LC Lin TY Tseng SC Wang TH Tsai 2007 Oral bioavailability of curcumin in rat and the herbal analysis from Curcuma longa by LC–MS/MS J Chromatogr B 853 183 189 https://doi.org/10.1016/j.jchromb.2007.03.010
8. K Xiong Y Zhang Q Wen J Luo Y Lu Z Wu B Wang Y Chen L Zhao S Fu 2020 Co-delivery of paclitaxel and curcumin by biodegradable polymeric nanoparticles for breast cancer chemotherapy Int J Pharm 589 119875 https://doi.org/10.1016/j.ijpharm.2020.119875
9. X Liu H Gan C Hu W Sun X Zhu Z Meng R Gu Z Wu G Dou 2019 Silver sulfadiazine nanosuspension-loaded thermosensitive hydrogel as a topical antibacterial agent Int J Nanomedicine 14 289 300 https://doi.org/10.1016/10.2147/IJN.S187918
10. I Khan K Saeed I Khan 2019 Nanoparticles: properties, applications and toxicities Arab J Chem 12 7 908 931 https://doi.org/10.1016/j.arabjc.2017.05.011
11. A Reeves SV Vinogradov P Morrissey M Chernin MM Ahmed 2015 Curcumin-encapsulating nanogels as an effective anticancer formulation for intracellular uptake MolCell Pharmacol 7 3 25 40 https://doi.org/10.1016/10.4255/mcpharmacol.15.04
12. MS Algahtani MZ Ahmad IH Nourein HA Albarqi HS Alyami MH Alyami AA Alqahtani A Alasiri TS Algahtani AA Mohammed J Ahmad 2021 Preparation and characterization of curcumin nanoemulgel utilizing ultrasonication technique for wound healing: in vitro, ex vivo, and in vivo evaluation Gels 7 213 https://doi.org/10.3390/gels7040213
13. D Laloo R Tahbildar K Smith A Ahmed J Nath D Shil G Das A Langbang SK Prasad NK Singh 2020 Impact of quality control standardization parameters and antioxidant potential of the aerial parts of potentilla fulgens wall: a comprehensive monographic study J Biol Act Prod Nat 10 4 338 356 https://doi.org/10.1080/22311866.2020.1806731
14. GE Trease WC Evans 2002 Pharmacognosy 15 Saunders Company London
15. H Wagner S Bladt EM Zgainsk 1984 Plant Drug Analysis: A Thin Layer Chromatography Atlas 2 Springer-Verlag Berlin Heidelberg, New York
16. HPS Makkar M Bluemmel NK Borowy K Becker 1993 Gravimetric determination of tannins and their correlations with chemical and protein precipitation methods J Sci Food Agric 61 161 165
17. LM Cordenonsi RM Sponchiado SC Campanharo CV Garcia RP Raffin EES Schapoval 2017 Study of flavonoids present in pomelo (Citrus maxima) by DSC, UV-vis, IR, 1H and 13C NMR and MS Drug Anal Res 1 31 37
18. A Bharali H Sarma N Biswas JM Kalita B Das BP Sahu SK Prasad D Laloo 2023 Green synthesis of silver nanoparticles using hydroalcoholic root extract of Potentillafulgensand evaluation of its cutaneous wound healing potential Mater Today Commun 35 106050 https://doi.org/10.1016/j.mtcomm.2023.106050
19. MS Blois 1958 Antioxidant determinations by the use of a stable free radical Nature 26 4617 1199 1200
20. R Gandhisan A Thamaraichelvan K Baburaj 1991 Anti-inflammatory action of Lanneacoromandelica HRBC membrane stabilization Fitoterapia 62 82 83
21. CA Anosike O Obidoa LUS Ezeanyika 2012 The anti- inflammatory activity ofgarden egg (Solanum aethiopicum) on egg albumin-induced oedemaand granuloma tissue formation in rats Asian Pac J Trop Med 5 1 62 66 https://doi.org/10.1186/2008-2231-20-76
22. BP Sahu MK Das 2014 Nanosuspension for enhancement of oral bioavailability of felodipine Appl Nanosci 4 2 189 197 https://doi.org/10.1007/s13204-012-0188-3
23. D Yuancai KN Wai H Jun S Shoucang BHT Reginald 2010 A continuous and highly effective static mixing process for antisolvent precipitation of nanoparticles of poorly water-soluble drugs Int J Pharm 386 256 261 https://doi.org/10.1016/j.ijpharm.2009.11.007
24. B Mandal KS Alexander AT Riga 2010 Sulfacetamide loaded eudragit RL100 nanosuspension with potential for ocular delivery J Pharm Pharmaceut Sci 13 4 510 523
25. S Jebril RKB Jenana C Dridi 2020 Green synthesis of silver nanoparticles using Meliaazedarach leaf extract and their antifungal activities: In vitro

and in vivo Mater Chem Phys 248 122898 https://doi.org/10.1016/j.matchemphys.2020.122898

26. KD Meypaul G Garg S Koul A Sharma 2020 Preparation and characterization of Curcumin based nanogel for topical anti-inflammatory activity Int J Adv Sci Technol 29 2 3424 3438

27. R Aiyalu A Govindarjan A Ramasamy 2016 Formulation and evaluation of topical herbal gel for the treatment of arthritis in animal model Braz J Pharm Sci 52 493 507 https://doi.org/10.1590/S1984-82502016000300015

28. NM Harish P Prabhu RN Charyulu MA Gulzar EV Subrahmanyam 2009 Formulation and evaluation of in situ gels containing clotrimazole for oral candidiasis Indian J Pharm Sci 71 4 421 427 https://doi.org/10.4103/0250-474X.57291

29. GNK Ganesh MK Singh S Datri VVSR Karri 2019 Design and development of curcumin nanogel for squamous cell carcinoma J Pharm Sci Res 11 4 1638 1645

30. M Ubaid S Ilyas S Mir AK Khan R Rashid MZU Khan ZG Kanwal A Nawaz A Shah G Murtaza 2016 Formulation and in vitro evaluation of carbopol 934-based modified clotrimazole gel for topical application An Acad Bras Cienc 88 4 2304 2317 https://doi.org/10.1590/0001-3765201620160162

31. A Choudhary V Kant BL Jangir VG Joshi 2020 Quercetin loaded chitosan tripolyphosphate nanoparticles accelerated cutaneous wound healing in Wistar rats Eur J Pharmacol 880 173172 https://doi.org/10.1016/j.ejphar.2020.173172

32. R Khullar D Kumar N Seth S Saini 2012 Formulation and evaluation of mefenamic acid emulgel for topical delivery Saudi Pharm J 20 1 63 67 https://doi.org/10.1016/10.1016/j.jsps.2011.08.001

33. NA Patel NJ Patel RP Patel 2009 Formulation and evaluation of curcumin gel for topical application Pharm Dev Technol 14 1 83 92 https://doi.org/10.1016/10.1080/10837450802409438

34. BP Sahu HK Sharma MK Das 2011 Development and evaluation of a mucoadhesive nasal gel offelodipine prepared with mucoadhesive substance of *Dillenia indica* L Asian J Pharm Sci 5 5 175 187

35. Savenije B, Strubbe J & Ritshes-Hoitinga M (2010) Nutrition, feeding and animal welfare. The Care and Management of Laboratory and Other Research Animals, 183–193.

36. MM Zangeneh Z Joshani A Zangeneh E Miri 2019 Green synthesis of silver nanoparticles using aqueous extract of Stachyslavandulifolia flower, and their cytotoxicity, antioxidant, antibacterial and cutaneous wound-healing properties Appl Organomet Chem 33 9 e5016 https://doi.org/10.1016/10.1002/aoc.5016

37. S Murthy MK Gautam S Goel V Purohit H Sharma RK Goel 2013 Evaluation of in vivo wound healing activity of Bacopa monniera on different wound model in rats Biomed Res Int 2013 972028 https://doi.org/10.1155/2013/972028

38. A Zanfirescu G Nitulescu G Stancov D Radulescu C Trif GM Nitulescu S Negres OT Olaru 2020 Evaluation of topical anti-inflammatory effects of a gel formulation with plantago lanceolata, achillea millefolium, aesculus hippocastanum and taxodium distichum Sci Pharm 88 2 26 https://doi.org/10.3390/scipharm88020026

39. C Heffernan M Ukrainczyk RK Gamidi BK Hodnett AC Rasmuson 2017 Extraction and purification of curcuminoids from crude curcumin by a combination of crystallization and chromatography Org Process Res Dev 21 6 821 826 https://doi.org/10.1021/acs.oprd.6b00347

40. AK Singh S Yadav K Sharma Z Firdaus P Aditi K Neogi M Bansal MK Gupta A Shanker RK Singh P Prakash 2018 Quantum curcumin mediated inhibition of gingipains and mixed-biofilm of *Porphyromonasgingivalis* causing chronic periodontitis RSC Adv 8 70 40426 40445 https://doi.org/10.1039/c8ra08435a

41. AM Anderson MS Mitchell RS Mohan 2000 Isolation of Curcumin from Turmeric J Chem Educ 77 3 359 360 https://doi.org/10.1021/ed077p359

42. D Quintanar-Guerrero E All'emann H Fessi E Doelker 1998 Preparation techniques and mechanisms of formation of biodegradable nanoparticles from preformed polymers Drug Dev Ind Pharm 24 1113 1128 https://doi.org/10.3109/03639049809108571

43. S Revathy S Elumalai M Benny A Benny 2011 Isolation, purification and identification of curcuminoids from turmeric (*Curcuma longa* L.) by column chromatography J Exp Sci 2 21 25

44. JO Arawande A Akinnusotu JO Alademeyin 2018 Extractive value and phytochemical screening of ginger (zingiberofficinale) and turmeric (curcuma longa) using different solvents Inst j tradit med 8 1 13 22

45. MR Dangat KC Mahajan VD Bhot AS Gawade 2019 Extraction and phytochemical screening of rhizomes of *Curcuma longa* Int J Pharm Sci Rev Res 59 2 18 20

46. N Deb P Majumdar AK Ghosh 2013 Pharmacognostic and phytochemical evaluation of the Rhizomes of *Curcuma longa* Linn J Pharma SciTech 2 2 81 86

47. KFM Opuni S Asare-Nkansah P Osei-Fosu A Akonnor SO Bekoe ANO Dodoo 2021 Monitoring and risk assessment of pesticide residues in selected herbal medicinal products in Ghana Environ Monit Assess 193 8 470 https://doi.org/10.1007/s10661-021-09261-1

48. GB Barbosa JMO Minguillan 2021 Antioxidant activity and total phenolic content of fresh and cured rhizomes of *Curcuma longa* and Etlingera philippinensis Int Food Res J 28 4 839 847

49. M Maizura A Aminah WM Wan Aida 2011 Total phenolic content and antioxidant activity of kesum (*Polygonum minus*), ginger (*Zingiberofficinale*) and turmeric (*Curcuma longa*) extract Int Food Res J 18 529 534

50. A Sahoo B Kar S Sahoo S Jena A Kuanar S Parameswaran J Patnaik S Nayak 2019 De Novo transcriptome sequencing explored cultivar specific sequence variation and differential expression of pigment synthesis genes in turmeric (*Curcuma longa* L.) Ind Crops Prod 134 388 402 https://doi.org/10.1016/j.indcrop.2019.04.021

51. M Suhaj 2006 Spice antioxidants isolation and their antiradical activity: a review J Food Compos Anal 19 531 537 https://doi.org/10.1016/j.jfca.2004.11.005

52. I Stoilova A Krastanov A Stoyanova P Denev S Gargova 2007 Antioxidant activity of a ginger extract (*Zingiberofficinale*) Food Chem 102 764 770 https://doi.org/10.1016/j.foodchem.2006.06.023

53. M Sökmen AM Khan 2016 The antioxidant activity of some curcuminoids and chalcones Inflammopharmacology 24 2–3 81 86 https://doi.org/10.1007/s10787-016-0264-5

54. ATN Vo TD Luu MNU Nguyen TV Vo W Duan PH Tran TT Tran 2017 Sonication-assisted nanoprecipitation in drug delivery Curr Drug Metab 18 2 145 156 https://doi.org/10.2174/1389200218666170116103555

55. P Shah P Desai A Patel M Singh 2012 Skin permeating nanogel for the cutaneous co-delivery of two anti-inflammatory drugs Biomaterials 33 5 1607 1617 https://doi.org/10.1016/j.biomaterials.2011.11.011

56. GK Jain SA Pathan S Akhter N Ahmad N Jain S Talegaonkar 2010 Mechanistic study of hydrolytic erosion and drug release behaviour of PLGA nanoparticles: influence of chitosan Polymer Degrad Stab 95 2360 2366 https://doi.org/10.1016/j.polymdegradstab.2010.08.015

57. AA Tehrani MM Omranpoor A Vatanara M Seyedabadi V Ramezani 2019 Formation of nanosuspensions in bottom-up approach: theories and optimization Daru 27 1 451 473 https://doi.org/10.1007/s40199-018-00235-2

58. Y Liu G Yang Z Da H Yue K Nigam APJ Middelberg Z Chun-Xia 2020 Formulation of nanoparticles using mixing-induced nanoprecipitation for drug delivery Ind Eng Chem Res 59 9 4134 4149 https://doi.org/10.1021/acs.iecr.9b04747

59. Fessi H, Puissieux F, Devissaguet JP, Thies C (1988) Process for the preparation of dispersible colloidal systems of a substance in the form of nanoparticles. US Patent US5118528-2 June

60. JM Barichello M Morishita K Takayama T Nagai 1999 Encapsulation of hydrophilic and lipophilic drugs in PLGA nanoparticles by the nanoprecipitation method Drug Dev Ind Pharm 25 471 476 https://doi.org/10.1081/DDC-100102197

61. A Oryan AT Naeini A Moshiri A Mohammadalipour M Tabandeh 2012 Modulation of cutaneous wound healing by silymarin in rats J Wound Care 21 9 457 464 https://doi.org/10.12968/jowc.2012.21.9.457

62. D Dwivedi M Dwivedi S Malviya V Singh 2017 Evaluation of wound healing, anti-microbial and antioxidant potential of Pongamiapinnata in Wistar rats J Tradit Complement Med 7 1 79 85 https://doi.org/10.1016/j.jtcme.2015.12.002

63. A Kundu A Ghosh NK Singh GK Singh A Seth SK Maurya S Hemalatha D Laloo 2016 Wound healing activity of the ethanol root extract and polyphenolic rich fraction from *Potentilla fulgens* Pharm Biol 54 11 2383 2393 https://doi.org/10.3109/13880209.2016.1157192

64. GF Caetano M Fronza MN Leite A Gomes MAC Frade 2016 Comparison of collagen content in skin wounds evaluated by biochemical assay and by computer-aided histomorphometric analysis Pharm Biol 54 11 2555 2559 https://doi.org/10.3109/13880209.2016.1170861

Sarma *et al. Future Journal of Pharmaceutical Sciences*   (2023) 9:85

Page 21 of 21

65. SA Guo LA DiPietro 2010 Factors affecting wound healing J Dent Res 89 3 219 229 https://doi.org/10.1177/0022034509359125

66. R Geethalakshmi C Sakravarthi T Kritika MA Kirubakaran D Sarada 2013 Evaluation of antioxidant and wound healing potentials of Sphaeranthusamaranthoides Burm Biomed Res Int https://doi.org/10.1155/2013/607109

67. TJ Koh LA DiPietro 2011 Inflammation and wound healing: the role of the macrophage Expert Rev Mol Med https://doi.org/10.1017/S1462399411001943

68. CJ Morris 2003 Carrageenan—Induced paw edema in the rat and mouse PG Winyard DA Willoughby Eds Methods in Molecular Biology: Inflammation Protocols Humana Press Inc Totowa 115 121

69. KR Patil UB Mahajan BS Unger SN Goyal S Belemkar SJ Surana S Ojha CR Patil 2019 Animal models of inflammation for screening of anti-inflammatory drugs: implications for the discovery and development of phytopharmaceuticals Int J Mol Sci 20 18 4367 https://doi.org/10.3390/ijms20184367

70. Y Peng M Ao B Dong Y Jiang L Yu Z Chen C Hu R Xu 2021 Anti-Inflammatory effects of curcumin in the inflammatory diseases: status, limitations and countermeasures Drug Des Devel Ther 15 4503 4525 https://doi.org/10.2147/DDDT.S327378

71. M Gera N Sharma M Ghosh DL Huynh SJ Lee T Min T Kwon DK Jeong 2017 Nanoformulations of curcumin: an emerging paradigm for improved remedial application Oncotarget 8 39 66680 66698 https://doi.org/10.18632/oncotarget.19164

72. HR Rahimi R Nedaeinia A SepehriShamloo S Nikdoust R KazemiOskuee 2016 Novel delivery system for natural products: Nano-curcumin formulations Avicenna J Phytomed 6 4 383 398

Publisher's Note